ARTICLES

Quartz family of silica polymorphs: Comparative simulation study of quartz, moganite, and orthorhombic silica, and their phase transformations

Vladimir V. Murashov
Department of Chemistry, Dalhousie University, Halifax, Nova Scotia, Canada B3H 4J3

Igor M. Svishchev
Department of Chemistry, Trent University, Peterborough, Ontario, Canada K9J 7B8
(Received 18 June 1997)

A quartz family of silica polymorphs is studied. The structure and phase transformations of quartz, moganite, and orthorhombic silica (*o*-silica) are examined using molecular dynamics simulations. Moganite and its high-pressure forms appear to be the most stable phases in the temperature range from 100 to 1100 K and the pressure range from 0 to 30 GPa. Upon applied pressure *o*-silica transforms first into a monoclinic phase (at about 15 GPa) and then into a high-density orthorhombic phase (at about 28 GPa). Moganite also exhibits two crystal-crystal phase transformations, at about 5 and 21 GPa. Quartz undergoes amorphization at approximately 21 GPa in accordance with previous studies. Moganite and *o*-silica are likely to be present among naturally occurring microcrystalline forms of silica; however, similarities in their x-ray-diffraction patterns would make it very difficult to distinguish between them. The implications of computer simulation results for crystal growth and metamorphism are discussed. [S0163-1829(98)00810-8]

INTRODUCTION

Silica can exist in a variety of crystalline forms which share the same building block-regular (or nearly regular) $[SiO_4]$ coordination tetrahedron.[1] These forms are typically three-dimensional network structures built of corner-shared $[SiO_4]$ units (among low-density polymorphs only the so-called silica-W contains chains of the edge-shared $[SiO_4]$ tetrahedra[2]). Silica forms are widespread in nature. Quartz is the second most abundant mineral in Earth's crust. Cristobalite and tridymite are less common, as well as melanophlogite, a rare low-density form, which is always found to contain some organic matter or sulfur acting as templating agents.[3] Several high-pressure polymorphs, including keatite,[4] coesite,[5] and stishovite,[6] were first identified in laboratory studies. The latter two have later been discovered to occur naturally.[7,8]

It is now well documented in experimental and theoretical (computer simulation) studies that silica structures can undergo a variety of displacive transformations which preserve tetrahedral $[SiO_4]$ coordination. Collective motions of coordination tetrahedra (such as tilting) do not require as much energy as their deformation (reconstruction).[9,10] Quartz and cristobalite are known to have low- and high-temperature forms (α and β, respectively) which differ only slightly in the relative orientations of the $[SiO_4]$ units. Tridymite has also been reported to exhibit various temperature-and pressure-induced displacive phase transformations.[11,12] At higher pressures the fourfold-coordinated silica structures tend to transform into phases containing Si atoms with higher coordination numbers (reconstructive transitions). One such phase, stishovite, features octahedral coordination of Si atoms.

This study focuses on quartz and two lesser-known quartzlike structures: moganite and orthorhombic silica (*o*-silica). Although quartz is the most common and well-studied polymorph of silica, its structure and phase behavior remain a subject of intense speculations.[13–17] One of the most interesting features of quartz is that it can undergo amorphization under applied pressure.[18] In particular, recent investigations have indicated the possible formation of a superstructure in quartz, prior to amorphization.[19]

It is not well known that there exist crystalline forms of silica structurally similar to quartz, yet rather different in their physical and chemical properties.[20–26] They were first reported more than a century ago. As early as 1892, Michel-Lévy and Munier-Chalmas noted abnormal optical properties and growth habits of some natural fibrous minerals of silica.[27] More recently, detailed x-ray investigations of various natural microcrystalline forms of silica, previously believed to be ordinary ''quartz,'' have uncovered subtle differences in their structures.[28] In their diffraction patterns many of these forms have been found to violate the threefold axis symmetry of the conventional hexagonal quartz structure and they have also exhibited doubled periodicity with respect to the quartz unit cell. In order to explain these features, a structure of moganite has been put forward.[29,30] Very recently, computer simulations have uncovered another distinct quartzlike form of silica, so-called *o*-silica,[31] which has yet to be experimentally verified. Both of these phases, moganite and *o*-silica, have not been thoroughly examined theoretically. It is the purpose of this computer simulation study to investigate the structure and phase transformations

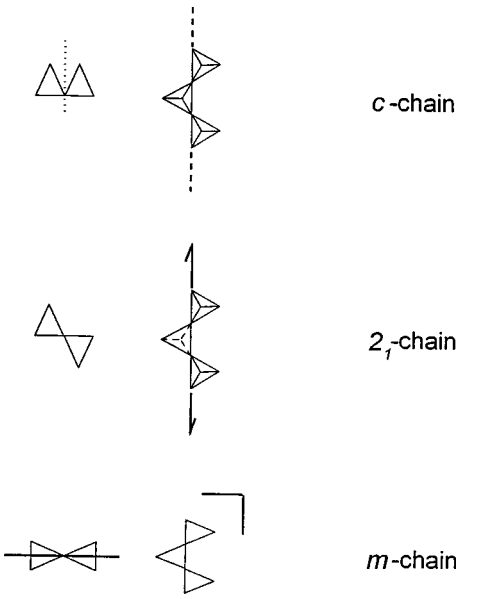

FIG. 1. Classification of tetrahedral chains found in silica structures.

of moganite and *o*-silica, and to compare them with those of hexagonal quartz. We also discuss the possible implications of our findings for crystal growth and metamorphism.

SIMULATION DETAILS

Computer simulations are now widely used in the studies of silica structures and their phase transformations.[32–38] In this molecular dynamics (MD) simulation study, we chose to work with the rigid-ion interatomic potentials developed by van Beest and co-workers.[34] Their force-field parameters are reasonably successful in describing the structural and dynamic properties of quartz. Variable-shape simulation cells containing 192 SiO_2 units were used. Nosé constant-pressure[39] and constant-temperature[40] algorithms were employed. In constructing the initial configurations of quartz and moganite, atoms were placed in the experimentally determined positions (see Refs. 41 and 29, respectively). In the case of *o*-silica, the structural information obtained in a previous MD simulation was used to set up its starting configuration.[31] A fourth-order Gear algorithm with a time step of 1 fsec was employed to integrate the equations of motion. The Ewald method was used to treat the long-range electrostatic interactions. Temperature and pressure were changed in steps of 50 K and 1 GPa, respectively. For each state point the systems were allowed to equilibrate for 5 psec, after which averages were accumulated over subsequent 5-psec trajectories.

RESULTS AND DISCUSSION

Quartz and quartzlike phases have framework structures, but for our purposes their packing patterns can be better described through consideration of tetrahedral chains.[31] We have found it convenient to classify tetrahedral chains in quartz and other silica structures according to their characteristic element of symmetry. This classification of tetrahedral chains is illustrated in Fig. 1. For example, tetrahedral chains comprising quartz can be designated as 2_1 chains. Their $[SiO_4]$ tetrahedra are linked according to twofold screw-axis symmetry. Tetrahedral chains that are found in feldspars and pyroxenes have a gliding plane with translation along the chain axis as a major element of symmetry. These arrangements can be denoted as *c* chains. Tetrahedral chains that are found in such silicates as Na_2SiO_3 and Li_2SiO_3 are symmetric about a mirror plane and can be described as *m* chains.

We first focus our attention upon moganite. The structure of moganite has been initially proposed to have orthorhombic $Ibam$ symmetry.[42] However, later studies involving Reitveld analysis of neutron and x-ray powder patterns have suggested lower monoclinic $I12/a1$ symmetry.[29] Our MD simulations indicate that at ambient conditions moganite has an orthorhombic $Ibam$ space group symmetry. Table I contains the structural data for moganite. This orthorhombic moganite (OM) features highly symmetric *m* chains. Figure 2(a) displays this structure viewed along the tetrahedral chains. At 300 K temperature and 5 GPa pressure, OM undergoes a reversible displacive transformation (with about a 4% volume change) into the lower-symmetry monoclinic structure [monoclinic moganite (MM)], which has been identified as having $I12/a1$ symmetry (see Table II). This phase transformation increases the lattice energy of the system, but due to the higher density of the monoclinic phase, the overall change in enthalpy during this transition is negative. These results indicate that both monoclinic and orthorhombic forms of moganite can have very similar enthalpies. The calculated metastability of the monoclinic form with respect to the orthorhombic form at ambient pressures either can be a manifestation of the deficiency of employed model or suggests that the experimental moganite structure refinement could have been done on the metastable high-pressure form, viz., monoclinic moganite.

TABLE I. Comparison of structures and energies for quartz family phases.

Quartz	Moganite	*o*-silica
$\sqrt{3}a=8.58(9)$ Å [8.510][a]	$c=8.89(2)$ Å [8.73(1)]	$a=8.68(1)$ Å
$2c=10.88(9)$ Å [10.810]	$b=10.50(5)$ Å [10.70(1)]	$b=10.31(1)$ Å
$a=4.94(7)$ Å [4.913]	$a=4.68(3)$ Å [4.87(1)]	$c=4.888(1)$ Å
$P3_12$	$Ibam$[b]	$Pbcn$
$\rho=2.60$ g/cm^3 [2.647]	$\rho=2.74$ g/cm^3 [2.63]	$\rho=2.74$ g/cm^3
ΔLE$=0.0$ kJ/mol	ΔLE$=-5.5$ kJ/mol	ΔLE$=3.3$ kJ/mol

[a]Experimental values are given in square brackets.

[b]Experimental data suggested the monoclinic $I12/a1$ form of moganite at ambient conditions.

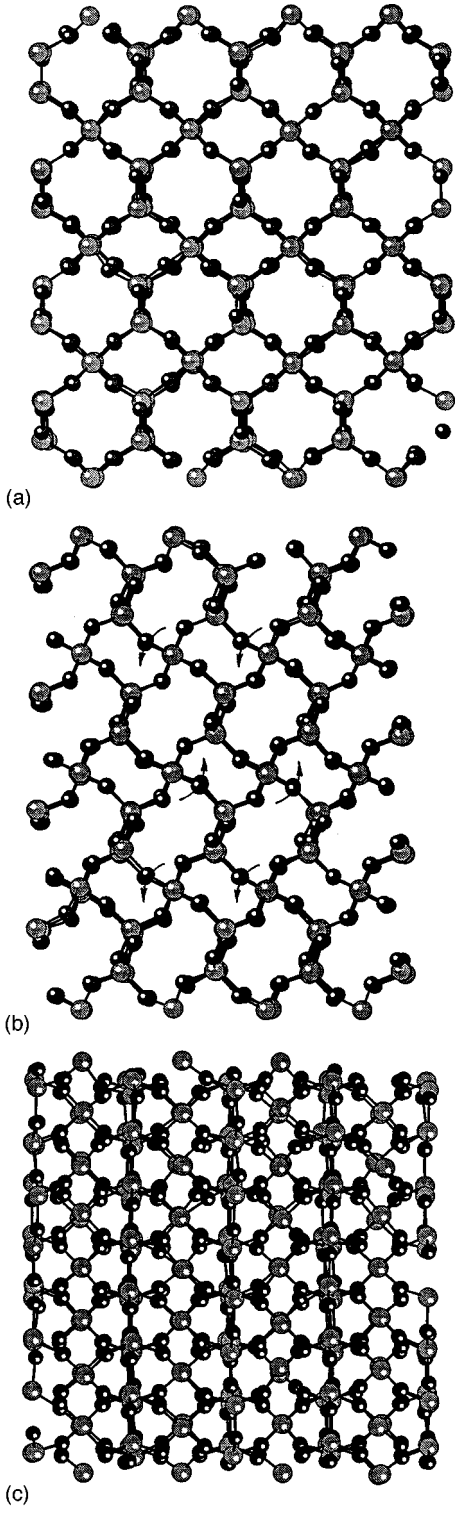

FIG. 2. View of the lower-density moganite forms: (a) along ⟨100⟩ of orthorhombic (OM) form; (b) along ⟨010⟩, and (c) along ⟨001⟩ of monoclinic (MM) form. Arrows indicate characteristic displacements of $[SiO_4]$ tetrahedra during compression.

Monoclinic moganite is composed of 2_1 chains and a view of moganite along these chains (along the ⟨010⟩ axis for the $I12/a1$ form) is identical to that of quartz along the ⟨1120⟩ axis [see Fig. 2(b)]. Unlike quartz, moganite features alternating fragments of both left- and right-handed threefold spirals cut by (101) planes. As a result, closed four-

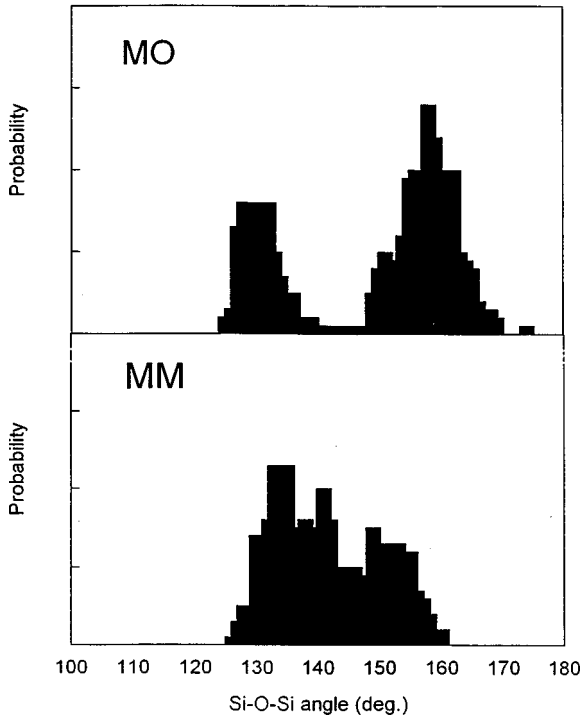

FIG. 3. The distributions of Si-O-Si angles in orthorhombic moganite (OM) and in monoclinic moganite (MM).

membered rings are present in moganite [see Fig. 2(b)], and the unit cell dimension doubles along the ⟨001⟩ of the quartz structure. Quartz, in comparison, has fourfold helical spirals propagating along twofold screw axes. Each four-membered ring in moganite shares a pair of opposing tetrahedra creating cross-linked chains. These four-membered rings are also found in coesite and feldspars. But those in moganite share $[SiO_4]$ tetrahedra, while those in coesite and feldspars are cross-linked through vertices of $[SiO_4]$ units. Interestingly, the projection of moganite perpendicular to the direction of chain propagation, e.g., along the ⟨001⟩ of MM [depicted in Fig. 2(c)], almost coincides with the corresponding projection of *o*-silica [see Fig. 2(b) in Ref. 31]. Both structures of moganite, orthorhombic and monoclinic, have Si-O radial distribution functions similar to that of quartz. The first maximum of this function for orthorhombic moganite appears around 1.62 Å (in quartz, the average Si-O distance is 1.61 Å). A slightly shorter Si-O distance of 1.61 Å for the first coordination sphere is found in monoclinic moganite at a pressure of 5 GPa. The Si-O-Si angle distribution in moganite, presented in Fig. 3, is markedly different from that in quartz [see Fig. 5(b) in Ref. 31]. In the orthorhombic form of moganite this distribution has two apparent maxima centered around 130° and 159°, whereas quartz exhibits a unimodal distribution of Si-O-Si angles centered at 144°. Monoclinic moganite features three maxima at about 135°, 141°, and 150°.

The structure of *o*-silica is built from *c* chains.[31] Close consideration of the packing pattern in *o*-silica reveals that it can be viewed as an extreme case of pyroxene,[43] where pyroxene tetrahedral chains (*c* chain) are interconnected by tetrahedrally coordinated silicon atoms instead of cations occupying oxygen polyhedra of higher-coordination numbers (compare the structures of clinopyroxene and orthorhombic

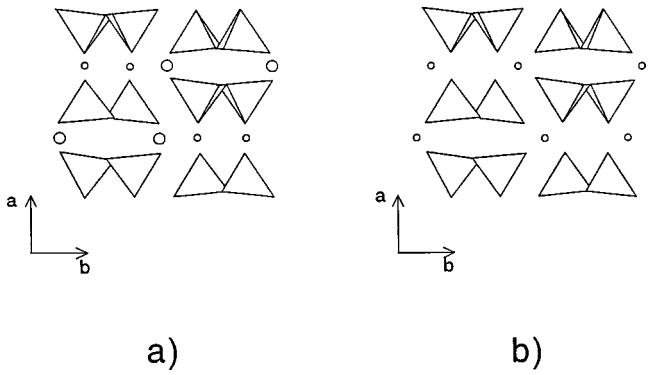

FIG. 4. View along ⟨001⟩ of (a) pyroxene and (b) *o*-silica.

silica in Fig. 4). The unit cell has orthorhombic $Pbcn$ symmetry (see Table I). The same space group symmetry and close unit cell parameters are found for protoenstatite,[44] $a=9.25$ Å, $b=8.74$ Å, and $c=5.32$ Å, where c chains are interconnected by Mg atoms. In *o*-silica silicon atoms occupy two distinct sites Si(1)($4c$) $x=0$, $y=0.293(3)$, $z=1/4$; Si(2)($8d$) $x=0.300(3)$, $y=0.414(1)$, $z=0.069(4)$; and oxygen atoms occupy three sites O(1)($8d$) $x=0.667(5)$, $y=0.463(1)$, $z=0.126(2)$; O(2)($8d$) $x=0.122(3)$, $y=0.375(2)$, $z=0.076(8)$; O(3)($8d$) $x=0.397(3)$, $y=0.295(1)$, $z=0.95(1)$. On the other hand, the unit cell dimensions of *o*-silica are close to those of moganite. In fact, both quartzlike structures, moganite and *o*-silica, have unit cells which can be derived from that of quartz by orthogonalization and doubling along the c dimension (see Table I).

We have simulated the compression of quartz, moganite, and *o*-silica up to 30 GPa at a temperature of 300 K. Quartz undergoes an amorphization around 21 GPa, which is in good agreement with results obtained in previous studies.[13] In a similar fashion to quartz, moganite reaches its limits of mechanical stability at about 21 GPa. Unlike quartz, moganite transforms into a crystalline phase with a monoclinic layered structure with an average coordination number for silicon of 5.33. Table II contains structural data for this phase denoted as MHP (moganite at high pressure). As mentioned earlier, moganite contains closed four-membered rings forming chains, while in quartz four-membered helical spirals are found. During the MM to MHP transition, cross-linking tetrahedra rotate symmetrically around twofold axes [see Fig. 2(b)]. Such motion shrinks the four-membered rings and brings rotating tetrahedra close to one of their four neighbors in the four-membered ring chain. The resulting high-pressure phase is composed of alternating layers of octahedral and tetrahedral zigzag chains as shown in Fig. 5(a). The former resemble those in the α-PbO_2 structure, and the latter are the remnants of the MM structure. Above 27 GPa, the tetrahedral chains gradually compress and twist, which results in the increase of the coordination number for silicon atoms from 4 to 6.

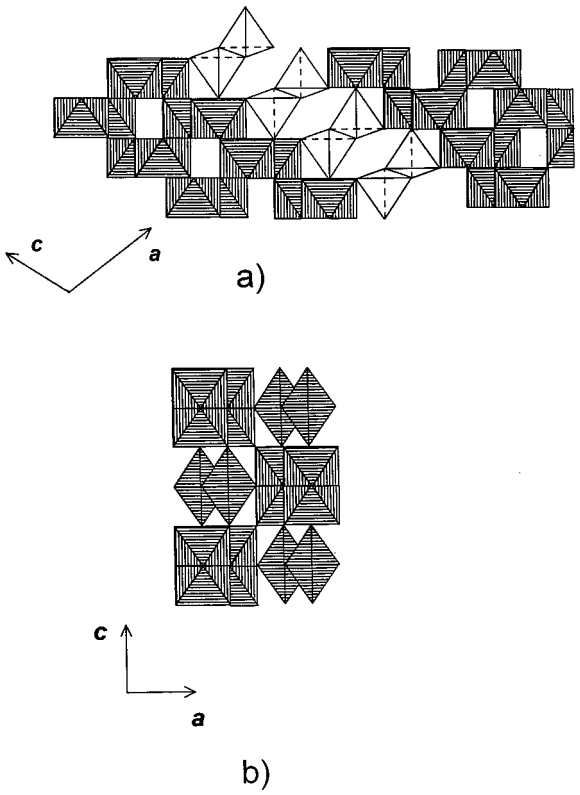

FIG. 5. High-pressure forms of (a) moganite and (b) *o*-silica. MHP and phase II are shown along the ⟨010⟩ direction.

Rather different behavior is exhibited by *o*-silica. The tetrahedral chains, c chains, in its structure are less compressible than the 2_1 and m chains in quartz and moganite. The average contraction of the *o*-silica lattice (the decrease in linear dimensions) along the direction of chain propagation

TABLE II. Structural data for high-pressure crystalline forms of silica found in this study. All results are at 300 K.

Structure	Pressure (GPa)	Unit cell parameters				Density (g/cm^3)	Space group symmetry
		a (Å)	b (Å)	c (Å)	β		
MM[a]	6	8.14(5)	4.57(2)	10.46(5)	90°	3.08	Monoclinic $I12/a1$
MHP[b]	21	10.12(9)	4.49(1)	6.30(2)	82°	4.18	Monoclinic $P2_1/c$
I	20	4.47(1)	8.13(1)	8.28(1)	86.8°	3.98	Monoclinic $P2_1$
II	28	7.94(1)	4.58(1)	7.72(1)	90°	4.46	Orthorhombic $Pbcm$

[a]Monoclinic moganite.

[b]Moganite at high pressure.

I: monoclinic phase obtained under pressure from *o*-silica.

II: orthorhombic form obtained by further compression of phase I.

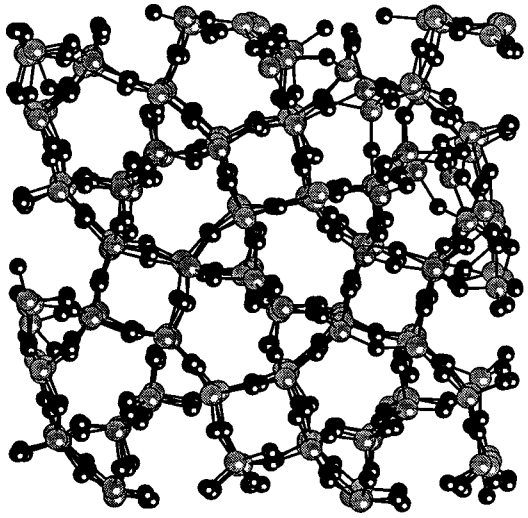

FIG. 6. Partially disordered phase recovered from crystalline phase II at ambient pressure.

is 0.19% per 1 GPa of applied pressure versus 0.78% for quartz and 0.60% for moganite in the pressure range from 0 up to 4 GPa. Apparently, internal strains build up faster in *o*-silica than in quartz or moganite, and *o*-silica becomes mechanically unstable at lower pressures. Under pressure, *o*-silica undergoes two phase transformations. The first phase transformation occurs at approximately 15 GPa and gives rise to a monoclinic phase, phase I. Table II contains its structural data, where the x axis corresponds to the z axis of *o*-silica, y to x, and z to y. This displacive transformation occurs through symmetric rotation of coordination tetrahedra around twofold screw axes (perpendicular to the direction of chain propagation), such that the c chains compress and their alternating tetrahedra apexes tilt toward each other. Silicon atoms move up and down alternatively. Such deformation increases the coordination number of the silicon atoms which link the tetrahedra to 5. Half of the silicon atoms in the tetrahedral chains now have coordination number 4, and the other half have coordination number 6. The change in coordination results in the contraction of the lattice along its $\langle 010 \rangle$ and $\langle 001 \rangle$ directions, yet without significant compression along $\langle 100 \rangle$.

The next transition is observed at 28 GPa, which brings the symmetry up to orthorhombic $Pbcm$ (phase II) and raises the coordination number to 6. The unit cell parameters of phase II are given in Table II, but now the x axis corresponds to the y axis of *o*-silica, y to z, and z to x. Silicon atoms occupy one eightfold site and one fourfold site of the unit cell. Structure II is composed of slabs of edge- and face-sharing oxygen octahedra. These slabs are interconnected through vertices. The spaces between slabs are filled with chains of edge-sharing octahedra [see Fig. 5(b)] formed by chains, which in the lower-density structure I have fourfold- and fivefold-coordinated silicon atoms. Slabs and

TABLE III. X-ray-diffraction patterns of quartz, moganite, and *o*-silica.

Quartz			Moganite[a]		*o*-silica		
hkil	*d* (Å)	I/I_0 (%)	*d* (Å)	I/I_0 (%)	*hkl*	*d* (Å)	I/I_0 (%)
			n/a		110	6.64	24
					020	5.16	6
			4.43	10			
			4.35	6	200	4.34	18
$10\bar{1}0$	4.26	19	4.26	6			
					111	3.94	20
					021	3.55	36
			3.38	52	220	3.32	40
$10\bar{1}1$	3.34	100	3.34	100	121	3.28	100
					130	3.20	4
			3.11	8	211	3.10	7
			2.88	5	310	2.79	29
					221	2.75	3
					131	2.67	6
$11\bar{2}0$	2.46	9	2.45	3	002	2.44	10
					311	2.42	3
					231,102	2.36	6
$10\bar{1}2$	2.28	9	2.28	8	112,041	2.28	4
$11\bar{2}1$	2.24	5	2.26	1	240,330	2.22	3
			2.18	1	400	2.17	3
$20\bar{2}0$	2.13	7	2.13	6	202	2.13	4
					212	2.09	4
			2.02	2	241,331	2.02	8
$20\bar{2}1$	1.981	5	1.981	2			
			1.959	1	132	1.941	1

[a]Reference 28.

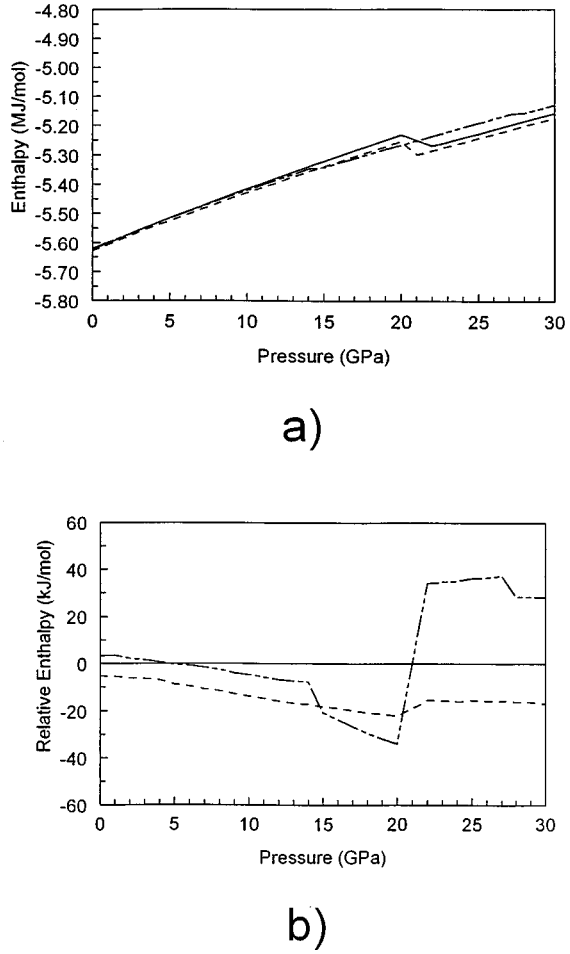

FIG. 7. The pressure dependence of (a) enthalpy and (b) relative enthalpy. The solid line represents quartz, the dashed line represents moganite, and the dotted line represents *o*-silica.

chains of octahedra in structure II propagate along the ⟨010⟩ direction.

We have simulated decompression of the high-pressure phase II from 30 GPa to ambient pressure. A partially disordered structure with a crystalline domain has been recovered (see Fig. 6). This structure is composed of *m* chains as in the orthorhombic form of moganite. In addition, these chains form hexagonal channels similar to those found in both quartz and moganite. The mirror planes of the tetrahedral chains are perpendicular to each other and alternate in two dimensions. As a result, these chains take part in the formation of deformed three-membered helical spirals (such helices are present in the quartz structure). The tetrahedra of these spirals form four-membered rings, similar to those in moganite.

One possible interpretation of these observations is that the partially disordered phase recovered from structure II is a hybrid of quartz and moganite. Thus *o*-silica can be expected to transform upon decompression into either quartz or moganite. We remark that in contrast with the high-to-low conversion of quartz requiring only a tilt of silica tetrahedra around twofold axes, the quartz-to-moganite or quartz–to–*o*-silica–to–moganite transformations would require more drastic alterations of the parent quartz structure. Such reconstructive solid-state phase transformations are very difficult to model in molecular dynamics simulation experiments.

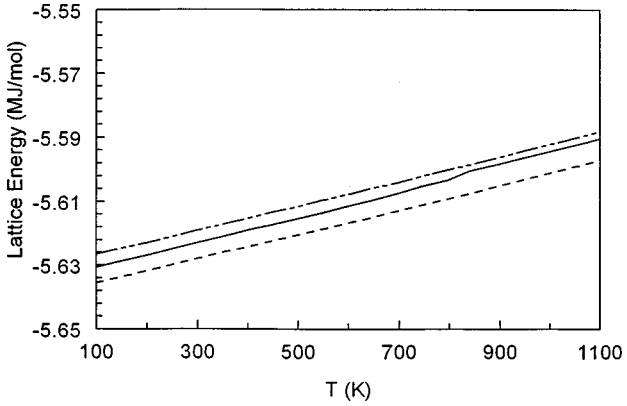

FIG. 8. Temperature dependence of the lattice energy for quartz, moganite, and *o*-silica at 0.1 GPa.

This can account for our inability to fully reproduce them in MD simulations.

It is worth noting that phase transitions between quartz and pyroxene forms have been observed experimentally for $LiAlSi_2O_6$.[45] The reversible transformation of the β-quartz form (with Al occupying Si sites of β-quartz and Li residing in the interstices) to spodumene (with Al and Li in octahedral sites of this monoclinic pyroxene) takes place in the pressure range 1–2.7 GPa. At pressures above 2.7 GPa, the pyroxene form is the most stable at all temperatures. At temperatures above 800 K and pressures between 0.1 and 0.9 GPa, the keatite form is stable. All three transitions are believed to be reversible.

IMPLICATIONS FOR CRYSTAL GROWTH AND METAMORPHISM

Our lattice energy (LE) calculations support the possible coexistence of all three phases, quartz, moganite, and *o*-silica in silica minerals. At ambient conditions (300 K and 0.1 MPa), the moganite phase appears to be somewhat more stable than quartz (its LE is lower by 5.5 kJ/mol), while *o*-silica is less stable than quartz (its LE is higher by 3.3 kJ/mol). For comparison, the calculated lattice energy for cristobalite is much higher than the lattice energy for quartz, viz., by 15.5 kJ/mol. These results concur with experimental solubility data[22,46] and explain the absence of the visible moganite-to-quartz transformation in water.[30] At the same time, the calculated stability of moganite over quartz at ambient conditions contradicts recently published thermodynamic data for moganite,[47] where moganite is reported to have an excess enthalpy of 3.4 kJ/mol. We might further speculate that the observed higher solubility of chalcedony,[22] as compared with quartz, is associated with the presence of *o*-silica, and not of moganite as previously thought. The presence of *o*-silica in some naturally occurring microcrystalline forms of silica can also account for their higher reactivity with alkalies. It has been suggested that this reaction plays an important role in the destruction of concretes (the first example can be found in a publication by Stanton[24] in 1940).[23]

In order to find the characteristic reflections identifying *o*-silica, we have calculated its x-ray-diffraction pattern. It is given in Table III along with experimental x-ray-diffraction

patterns of quartz and moganite. Both diffraction patterns of *o*-silica and moganite accommodate main reflections of quartz and differ from each other in minor reflections. Therefore, it would be very difficult to distinguish reflections due to individual quartzlike phases from powder x-ray-diffraction patterns of their mixtures. We might, for instance, speculate that one of the phenotypes of ''moganite,'' either massive chertlike rocks[20] or white powders surrounding nodules,[30] contains *o*-silica.

Our enthalpy calculations (see Fig. 7) suggest that moganite and its high-pressure forms may be more stable than quartz and its amorphous form in the whole range of pressures up to 30 GPa. These calculations also indicate that *o*-silica may become more stable than quartz at pressures higher than 5 GPa, but not above 21 GPa when quartz undergoes amorphization.

Our molecular dynamics calculations at atmospheric pressure (Fig. 8) show that neither moganite nor *o*-silica undergo an α-to-β phase transformation in the temperature range from 100 to 1100 K, while quartz does show such a transformation at about 800 K. It appears that moganite has the lowest lattice energy, while *o*-silica has the highest in this range of temperature. After quartz transforms to its high-temperature form, the lattice-energy difference between β-quartz and *o*-silica reduces to 2 kJ/mol. This suggests that under equilibrium conditions moganite should grow from melts and hydrothermal fluids, and mineralogical data to indicate a widespread occurrence of moganite among microcrystalline forms of silica.[30]

Some fibrous forms of silica containing quartzlike phases were found to grow along the $\langle 1120 \rangle$ direction of quartz, while quartz crystals are usually elongated along $\langle 001 \rangle$. This experimental observation is in agreement with the expected growth of both moganite and *o*-silica along the direction of tetrahedral chains. One might suggest that moganite would preferentially grow under conditions supporting the formation of $(\text{-Si-O-})_2\text{Si}(\text{-O-Si-})_2$ chain fragments, as it is a peculiar arrangement for this structure. The formation of *o*-silica could be expected to proceed from hydrothermal solutions at elevated pressures in the presence of metal ions and under conditions supporting the linearity of siloxane chains (e.g., Prassas *et al.* have demonstrated that the presence of Na^+ ions promotes linear chain formation[48]). Indeed, Heaney and Post have noted the association of ''unusual'' quartz forms with sodium cations.[30] It has been shown that fibrous silica precipitates from slightly saturated aqueous solutions (weak polymerization) at relatively low temperatures ($<100\,^\circ$C), which promotes the assembly of pyroxene-chain polymers via bridging silica monomers.[49] Therefore, the pyroxenelike arrangement could become kinetically favorable under such hydrothermal conditions. We propose using a pyroxene cut along the (001) plane as a possible substrate in the synthesis of *o*-silica. We also suggest looking for *o*-silica among minerals containing pyroxenes.

It is worth mentioning that the formation of quartzlike phases is not a prerogative of silica. Germania, GeO_2, the structural analog of silica, has been shown to crystallize easily into fibrous forms by quenching from a high-temperature aqueous solution.[50] The physical, chemical, and structural properties of the products were analogous to those of the fibrous silica forms. Due to the reported simplicity of this synthesis, germania could be another candidate to study the quartz family of structures.

CONCLUSIONS

Using MD simulations, we have examined the structure and phase transformations of quartz and two quartzlike polymorphs, *o*-silica and moganite. Upon applied pressure, both *o*-silica and moganite exhibit a series of crystal-crystal transformations, while quartz undergoes amorphization. Unlike quartz, moganite and *o*-silica do not demonstrate the temperature-induced α-β transformation. Thermodynamic calculations suggest the possible coexistence of quartz, moganite, and *o*-silica in naturally occurring minerals. However, similarities in their x-ray-diffraction patterns would make it extremely difficult to distinguish between them. It is interesting to note that among these phases moganite has the lowest enthalpy in the entire examined range of temperatures and pressures, up to 1100 K and 30 GPa.

ACKNOWLEDGMENTS

V.V.M. would like to thank the Killam Trustees for support and Professor M. A. White for comments about this work.

[1] A. F. Wells, *Structural Inorganic Chemistry*, 3rd ed. (Oxford University Press, London, 1962).
[2] A. Weiss and A. Weiss, Z. Anorg. Allg. Chem. **276**, 95 (1954).
[3] B. J. Skinner and D. E. Appleman, Am. Mineral. **48**, 854 (1963).
[4] P. P. Keat, Science **120**, 328 (1954).
[5] L. Coes, Jr., Science **118**, 131 (1953); T. Araki and T. Zoltai, Z. Kristallogr. **129**, 381 (1969).
[6] S. M. Stishov and S. V. Popova, Geokhimiya **1961**, 837.
[7] E. C. T. Chao, Foote-Prints **32**, 25 (1960).
[8] E. C. T. Chao, J. J. Fahey, J. Littler, and D. J. Milton, J. Geophys. Res. **67**, 419 (1962).
[9] N. J. Henson, A. K. Cheetham, and J. D. Gale, Chem. Mater. **6**, 1647 (1994).
[10] K. de Boer, A. P. J. Jansen, and R. A. van Santen, Phys. Rev. B **52**, 12 579 (1995).
[11] H. Graetsch and O. W. Flörke, Z. Kristallogr. **195**, 31 (1991).
[12] R. L. Withers, J. G. Thompson, Y. Xiao, and R. J. Kirkpatrick, Phys. Chem. Miner. **21**, 421 (1994).
[13] J. S. Tse and D. D. Klug, Phys. Rev. Lett. **67**, 3559 (1991).
[14] J. R. Chelikowsky, H. E. King, Jr., and J. Glinnemann, Phys. Rev. B **41**, 10 866 (1990); N. Bingelli, N. R. Keskar, and J. R. Chelikowsky, *ibid.* **49**, 3075 (1994).
[15] G. W. Watson and S. C. Parker, Phys. Rev. B **52**, 13 306 (1995).
[16] V. V. Murashov, Phys. Rev. B **53**, 107 (1996).
[17] D. J. Lacks and R. G. Gordon, J. Geophys. Res. (Solid Earth) **98**, 22147 (1993).

[18] R. J. Hemley, A. P. Jephcoat, H. K. Mao, L. C. Ming, and M. H. Manghnani, Nature (London) **334**, 52 (1988).
[19] K. J. Kingma, R. J. Hemley, H. K. Mao, and D. R. Veblen, Phys. Rev. Lett. **70**, 3927 (1993).
[20] O. W. Flörke, J. B. Jones, and H. U. Schmincke, Z. Kristallogr. **143**, 156 (1976); G. Miehe, H. Graetsch, and O. W. Flörke, Phys. Chem. Miner. **10**, 197 (1984).
[21] O. F. Tuttle, Am. Mineral. **34**, 723 (1949).
[22] R. O. Fournier and J. J. Rowe, Am. J. Sci. **264**, 685 (1966); R. O. Fournier, in *Proceedings of the Symposium on Hydrogeochemistry and Biogeochemistry*, Tokyo, Japan, 1970, edited by E. Ingerson (The Clarke Company, Washington, D.C., 1973), Vol. I, p. 122.
[23] L. Bean and J. J. Tregoning, J. Am. Concrete Inst. **41**, 37 (1944).
[24] Stanton, Proc. Am. Soc. Civil Eng. **66**, 1781 (1940).
[25] A. Lacroix, C. R. Acad. Sci. **130**, 430 (1900).
[26] C. R. Pelto, Am. J. Sci. **254**, 32 (1956).
[27] A. Michel-Lévy and C. P. E. Munier-Chalmas, Bull. Soc. Fr. Mineral. **15**, 159 (1892).
[28] H. Graetsch, O. W. Flörke, and G. Miehe, Phys. Chem. Miner. **14**, 249 (1987).
[29] G. Miehe, H. Graetsch, O. W. Flörke, and H. Fueβ, Z. Kristallogr. **182**, 183 (1988).
[30] P. J. Heaney and J. E. Post, Science **255**, 441 (1992).
[31] I. M. Svishchev, P. G. Kusalik, and V. V. Murashov, Phys. Rev. B **55**, 721 (1997).
[32] C. R. A. Catlow and G. D. Price, Nature (London) **347**, 243 (1990).
[33] M. J. Sanders, M. Leslie, and C. R. A. Catlow, J. Chem. Soc. Chem. Commun. **1984**, 1271 (1984); J. Purton, R. Jones, C. R. A. Catlow, and M. Leslie, Phys. Chem. Miner. **19**, 392 (1993).
[34] B. W. H. van Beest, G. J. Kramer, and R. A. van Santen, Phys. Rev. Lett. **64**, 1955 (1990); G. J. Kramer, N. P. Farragher, B. W. H. van Beest, and R. A. van Santen, Phys. Rev. B **43**, 5068 (1991).
[35] A. C. Lasaga and G. V. Gibbs, Phys. Chem. Miner. **14**, 107 (1987); **16**, 29 (1988).
[36] S. Tsuneyuki, M. Tsukada, H. Aoki, and Y. Matsui, Phys. Rev. Lett. **7**, 869 (1988).
[37] P. F. McMillan and A. C. Hess, Phys. Chem. Miner. **17**, 97 (1990).
[38] J.-R. Hill and J. Sauer, J. Phys. Chem. **98**, 1238 (1994).
[39] M. Parinello and A. Rahman, J. Appl. Phys. **52**, 7182 (1981).
[40] W. G. Hoover, Phys. Rev. A **31**, 1695 (1985).
[41] R. W. G. Wyckoff, *Crystal Structures*, 2nd ed. (Wiley, New York, 1963).
[42] G. Miehe, O. W. Flörke, and H. Graetsch, Fortschr. Mineral **64**, 117 (1986).
[43] *Pyroxenes and Amphiboles: Crystal Chemistry and Phase Petrology*, Special Paper No. 2, edited by J. J. Papike (Mineralogical Society of Americda, Washington, DC, 1969).
[44] J. V. Smith, Acta Crystallogr. **58**, 515 (1959).
[45] J. L. Munoz, in *Pyroxenes and Amphiboles: Crystal Chemistry and Phase Petrology* (Ref. 43), p. 203.
[46] J. V. Walther and H. C. Helgeson, Am. J. Sci. **277**, 1315 (1977).
[47] I. Petrovic, P. J. Heaney, and A. Navrotsky, Phys. Chem. Miner. **23**, 119 (1996).
[48] M. Prassas, J. Phalippou, L. L. Hench, and J. Zarzycki, J. Non-Cryst. Solids **48**, 79 (1982).
[49] P. J. Heaney, Contrib. Mineral. Petrol. **115**, 66 (1993).
[50] J. F. White, E. R. Shaw, and J. F. Corwin, Am. Mineral. **43**, 580 (1958).